

On the Hyperparameters influencing a PINN’s generalization beyond the training domain

Andrea Bonfanti^{1,2,3}, Roberto Santana², Marco Ellero^{3,4,5}, Babak Gholami¹

⁽¹⁾BMW Group, Digital Campus Munich, Munich, Germany;

⁽²⁾University of the Basque Country (UPV/EHU), San Sebastian–Donostia, Spain;

⁽³⁾BCAM - Basque Center for Applied Mathematics, Bilbao, Spain;

⁽⁴⁾IKERBASQUE, Basque Foundation for Science, Bilbao, Spain;

⁽⁵⁾Zienkiewicz Centre for Computational Engineering (ZCCE), Swansea University, Swansea, UK.

Abstract. Physics-Informed Neural Networks (PINNs) are Neural Network architectures trained to emulate solutions of differential equations without the necessity of solution data. They are currently ubiquitous in the scientific literature due to their flexible and promising settings. However, very little of the available research provides practical studies that aim for a better quantitative understanding of such architecture and its functioning. In this paper, we analyze the performance of PINNs for various architectural hyperparameters and algorithmic settings based on a novel error metric and other factors such as training time. The proposed metric and approach are tailored to evaluate how well a PINN generalizes to points outside its training domain. Besides, we investigate the effect of the algorithmic setup on the outcome prediction of a PINN, inside and outside its training domain, to explore the effect of each hyperparameter. Through our study, we assess how the algorithmic setup of PINNs influences their potential for generalization and deduce the settings which maximize the potential of a PINN for accurate generalization. The study that we present returns insightful and at times counterintuitive results on PINNs. These results can be useful in PINN applications when defining the model and evaluating it.

Keywords: Physics-Informed Neural Networks · Differential Equations · Generalization

1 Introduction

Physics-Informed Neural Networks (PINNs) were first introduced in the 90s [1, 2] as an alternative method to solve ordinary and partial differential equations, based on the structure and approximation capabilities of Neural Networks. In late 2017, Raissi et al. reintroduced such architecture with the aforementioned name in two publications [3, 4], aimed at investigating its range of applicability to PDE-based forward and inverse problems. The analysis provided in those papers shows that PINNs are capable of solving classical monodimensional and bidimensional PDEs with little training effort and with satisfying precision. However, the complexity of the training routine rapidly increases if the underlying equations become more complex or the domain of the solution is large and/or multidimensional.

There are several reasons behind the choice of a Machine Learning-based approach, such as PINNs, instead of a classical numerical method to solve a PDE. A PINN architecture represents a simple and meshless solution that does not require high-level knowledge of the underlying equations and allows noisy data to be incorporated into the process, enabling the analysis of an incomplete set of data or partially understood phenomena [5]. On the other hand, especially due to their recent introduction in the field, PINNs lack the convergence guarantees that are characteristic of well-founded numerical solvers. Moreover, training a PINN can often be slow and sometimes unreliable for relatively complex equations in three or more dimensions [6]. That is, there is no certainty that a trained PINN reaches the correct

solution, and sometimes including data in the training process might be necessary to obtain a reasonable output [7]. Despite their drawbacks, PINNs have already seen their applications for a large variety of fields ranging from biology [8, 9], meteorology [10], and safety [11]. They are ubiquitous in recent research literature in general, due to the endless potential fields of applications. We refer the reader to [12] for a more detailed overview.

In this paper, we shed light on the generalization limitations of PINNs and hereinafter evaluate their generalization potential with respect to the training hyperparameters of the network architecture. In machine learning, generalization refers to the ability of a model to accurately predict far from the data used for training. Generalization has a particular connotation for PINNs, since the models are not expected to be used in regions where the loss function is not evaluated during training. Therefore, the concept of generalization of PINNs has not been investigated in depth in the literature. The outcome and contribution of our investigation lead to a more suitable algorithmic setup for PINNs to ensure a good generalization potential, along with a showcase of the effects of each hyperparameter on the predictions. For this purpose, we define a specific metric to quantify the generalizability of a PINN based on the algorithmic setup adopted. Our paper is structured as follows: In Section 2, we provide a formal definition of the PINN architecture and define our new generalization error metric after discussing the concept of generalization studied in this paper. Then, in Section 3, we perform a preliminary numerical analysis on the PINN architecture, to introduce the test case adopted for the rest of the paper and highlight the potential and limitations of PINNs. Section 4 is then devoted to illustrating the results obtained and validating them through statistical tests. The results are finally discussed in detail in Section 5 and the paper concludes with Section 6, which wraps up the main insights obtained through the experiments and provides recommendations for related future research directions.

1.1 Related work and Contributions

The analysis carried out in this paper is related to the generalization potential of neural networks, which consists of the capacity of a learning machine to evaluate correctly data samples that were not included in the training process. Generalization is a key property of machine learning algorithms as it indicates how well a trained model learns the input-output correlation for the considered dataset. In recent years, the generalization potential of neural networks has gained increasing interest in the research community due to its atypical behavior in the overparametrized regime given by the double descent curve [13–15]. Despite the availability of several results in this field, such analysis is not easily applicable to the case of PINN architectures. Indeed, the goal of PINN is to learn a specific analytical function that is unique for the majority of the problems. Henceforth, applying the aforementioned probabilistic bounds does not provide exact information on the accuracy of a PINN, which is an essential result for any kind of engineering application. To the best of our knowledge, the only applicable bounds are found in the work of Mishra et al. [16] which focuses on deriving error estimates of trained PINN architectures, based on the value of the loss function obtained and the number of sample points included in the training domain. However, the only applicable bound grows exponentially with respect to the distance from the training domain, which means that the error of a PINN can be arbitrarily large when evaluated far away from the boundaries of the training area.

Investigating the characteristics of the error of a PINN outside of its training domain has been scarcely explored in the literature. Indeed, since no knowledge of points outside the training domain is given to the PINN architecture during training, it is natural to assume that a valid prediction cannot be guaranteed. The majority of the works in the literature that presented PINN predictions outside of their training domain were focused on domain decomposition, as for the case of *hp*-VPINNs [17] and Finite-Basis-PINNs [18]. In both publications, the paradigm of training a PINN to solve a PDE in its domain is enhanced by training several PINN architectures to solve the PDE on some predefined subdomains of the original domain. By doing so, each PINN has to learn a simpler function, which makes the training process typically faster and more reliable. However, the prediction of each of the PINNs employed is neglected outside of its respective subdomain. Therefore, the prediction outside the training area is actually not used for predictions, but rather showcased to the reader for visualization purposes.

Instead of proving analytical bounds for errors in predictions far from the training domain of a PINN, our goal is to numerically study the degradation of the predictions of a PINN close to the boundaries of the training domain. The goal is then to identify which algorithmic components of PINNs can relieve the aforementioned degradation and therefore represent more suitable settings for applying a PINN. In line with the approach followed in this publication, we can find similar works, for instance, [19] and [20], which provide an analysis of the performance of PINNs based on several hyperparameters of the architecture, or [22], which studies the effect of different sampling strategies when choosing the training data for PINNs. Another similar project is given by [23], where a new methodology proposed to train PINNs is analyzed through the lenses of the depth and width of the neural network used.

The analysis we provide in this paper differs from previous works in some aspects:

- We make an extensive investigation on the effect of varying some of the most influential hyperparameters of the PINN algorithm and discuss the effect based on recent results from the scientific literature;
- We make use of statistical tests to validate and quantify the significance of the impact of the studied hyperparameters on the prediction of the network;
- We define a brand new metric to evaluate the goodness of generalization of arbitrary machine learning architectures that aim to overfit results, such as PINNs, and apply it to the aforementioned architecture.

The most relevant contribution is identified by the metric considered to evaluate the goodness of the algorithmic setup. Indeed, the classical relative L^2 error used to analyze the goodness of a PINN can be tuned by increasing the number of training epochs or using different learning strategies. On the other hand, our metric is constructed to be only slightly affected by stochasticity and is based on the intrinsic properties of the structure of a neural network and its natural ability to generalize outside the training domain.

2 Physics-Informed Neural Networks and Generalization

This Section introduces the theoretical background on which this paper is based. First, we provide a brief definition of a PINN and highlight the aspects of this neural network that are relevant to our study. Thereinafter, we focus on the concept of generalization for a PINN: we

explain why the concept does not apply to a PINN algorithm in a straightforward manner and introduce a possible method to study it.

2.1 Physics-Informed Neural Networks

The structure of a PINN is rather straightforward. The concept is to use a classical deep neural network to approximate the solution of a PDE in the domain where it is defined or where its values are needed. No a priori knowledge of the correct solution is necessary to train the model, except for its values at the boundaries of the domain and/or the initial condition of the PDE to make the problem well-posed. In the interior of the domain, where the solution is unknown, the network trains by minimizing the residuals of the underlying PDEs, computed through automatic differentiation. By doing so, the network tries to simultaneously mimic a function that fits the solution for the boundary and/or initial condition and a function that is mathematically coherent with the underlying PDEs. Therefore, if the accuracy obtained after training is good enough, the neural network will become an approximation of the PDE solution in the domain of interest.

Formally, let us consider the problem of finding a function $u : \Omega_T \rightarrow \mathbb{R}^n$ which solves a system of potentially non-linear partial differential equations, which we denote with \mathcal{F} , and which satisfies some initial and/or boundary conditions in some subdomain, which we will denote as $\Omega_T \subseteq \Omega \subset \mathbb{R}^d$. Finding the function u amounts to solving the system of equations shown in Equation (1).

$$\begin{cases} \mathcal{F}[u(\mathbf{x}, t)] = 0 & \forall (\mathbf{x}, t) \in \Omega_T \\ u(\mathbf{x}, t) = u_b(\mathbf{x}, t) & \forall \mathbf{x} \in \partial\Omega_T \\ u(\mathbf{x}, 0) = u_0(\mathbf{x}) & \forall \mathbf{x} \in \Omega_T \end{cases} \quad (1)$$

With u_b and u_0 being respectively equal to the value of u on $\partial\Omega_T$ and $\Omega_T \cap \{(\mathbf{x}, t) | t = 0\}$. To solve the above system with a traditional PDE solver, the domain Ω_T has to be discretized through a mesh first, then the equation must be solved in discrete settings on the said mesh. Instead, u can be approximated with a neural network $u_\theta : \Omega \rightarrow \mathbb{R}^d$ of parameters $\theta \in \mathbb{R}^{N_\theta}$, with N_θ representing the number of parameters of the architecture to be optimized. Therefore, the problem of solving the PDE becomes equivalent to finding the values of θ which make u_θ approximate u with a prescribed accuracy in Ω_T . Finding those values requires the usage of a set of N so-called ‘‘collocation points’’ $\{(\mathbf{x}_i, t_i)\}_{i=1}^N$. Collocation points are typically randomly sampled points that belong to Ω_T and indicate where the residuals of the equations \mathcal{F} are penalized, and a set of N_b points in $\partial\Omega_T$ that represent the boundary and initial conditions satisfied by u .

The network u_θ is referred to as ‘‘Physics-Informed’’ since its goal is to fit the values at the border while being skewed to minimize residuals of the equations represented by the functional \mathcal{F} . The typical loss function used for a Physics-Informed neural network is expressed in Equation (2).

$$\mathcal{L}(\theta, \{(\mathbf{x}_i, t_i)\}_{i=1}^N, \{(\mathbf{x}_j, t_j)\}_{j=1}^{N_b}) = \sum_{i=1}^N \|\mathcal{F}[u_\theta(\mathbf{x}_i, t_i)]\|^2 + \sum_{j=1}^{N_b} \|u_\theta(\mathbf{x}_j, t_j) - u(\mathbf{x}_j, t_j)\|^2 \quad (2)$$

It is clear from the definition of \mathcal{L} that its minimizer is the correct solution of the PDE, assuming that the problem is well-posed. However, learning the analytically exact solution with a neural network is practically cumbersome and theoretically infeasible due to limited machine precision. The solution u_θ obtained after training only aims to minimize its loss function in the points sampled before the training, included in some domain $\Omega_T \subseteq \Omega$. Once the training is done successfully, it is possible to accurately predict the value of u everywhere in Ω_T . This is possible thanks to the continuity of the target function and the generalization power of neural networks.

2.2 What is Generalization for a PINN and how to measure it?

The concept of generalization for an arbitrary machine learning architecture refers to its ability to provide accurate outputs when the input data is not that which was used to train the model. Neural networks are widely known to present a natural tendency to generalize well to unseen data samples. This property of neural networks is what allows PINNs to learn the target PDE solution everywhere by using scattered points in the domain Ω_T . The PINN does not have access to the true PDE solution at those points but, nevertheless, it can use them to learn the target function since it just needs to minimize the equation residuals. Those points can be interpreted as the dataset used by a PINN, and they roughly represent the domain Ω_T rather than the target PDE.

Once the model is trained, one can evaluate the accuracy of the PINN with some new locations in Ω_T . However, the accuracy obtained does not indicate the generalization potential of the model, since it is usually evaluated through new locations in Ω_T where the points used during training are dense. Therefore, a more suitable way to evaluate the generalization error made by a PINN can be given by studying the behaviour of its output outside of the convex hull defined by the training points. Indeed, u_θ is supposed to accurately approximate u inside Ω_T but there is no guarantee that the provided approximation is also valuable in $\Omega \setminus \Omega_T$, where u evolves through its analytical extension, even though the neural network has no information regarding points outside the training domain and cannot be expected to reproduce exactly the analytical solution everywhere.

However, we first need to select a metric to evaluate the potential of PINNs to predict outside Ω_T . To study the generalization potential of PINNs, we define and use the value G_l^ϵ , which we will refer to as “Generalization Level” (G_l). The chosen metric must be affected as little as possible by the stochasticity intrinsic to the training of a neural network. Indeed, we want to expect high GL values to indicate a more suitable structural choice for a PINN.

Consider the set of parameters of a PINN to be $\{\theta_i\}_{i=1}^{N_\theta} \in \Theta \subseteq \mathbb{R}^{N_\theta}$, and the remaining hyperparameters of the algorithm to be collected in an additional variable $H \in \mathcal{H}_{\text{PINN}}$. Consider also u_θ to identify a PINN initialized and trained according to the hyperparameters H and with trainable parameters in Θ . We define the GL of the hyperparameters of a PINN as in Definition 3.

$$G_l^\epsilon(\Theta, H) = \min_{u_\theta} \left\{ \max_{\Omega_G \subseteq \Omega \setminus \Omega_T} \{l(\Omega_G) \mid \text{s.t.} : \|u(x) - u_\theta(x)\| \leq \epsilon \quad \forall x \in \Omega_G\} \right\} \quad (3)$$

Here, the function l represents the area – length for one-dimensional cases – of the domain Ω_G , while ϵ is a constant threshold defined by the underlying problem. Therefore, G_l takes as

input the space of the parameters Θ and the hyperparameters used for training a PINN and outputs the biggest area outside the training domain in which the error remains bounded by ϵ for all the networks. This metric can be considered as the length of the x -segment outside of the training domain in which no variability can be visible and the prediction is accurate. The value of G_l depends on the structure and dimensionality of Θ and on the values of $H \in \mathcal{H}_{\text{PINN}}$, which in this paper are considered as $H = (N_{\text{CP}}, A)$: the number of collocation points N_{CP} , and the size of the training domain A .

Parameters influencing the potential in generalization It is reasonable to ask whether this extrapolation potential is affected by some of the hyperparameters of the neural network or the algorithmic setup of the PINN training. Among the possibly influential parameters, we consider the most relevant to be the following ones:

- **Network complexity:** The number of neurons and the number of layers used for the neural network supposed to mimic the solution of the chosen PDE.
- **Collocation points:** The number of reference locations in the PDE domain considered to compute the loss function of the PINN during training.
- **Domain size:** The size of the domain Ω_T where the PINN is trained to solve the PDE.

There are also other components of the PINN architecture that can influence the behavior of the solution outside the training domain. For instance, the type of activation function used in the architecture deeply affects the nature of the prediction of a PINN outside its training domain. The same holds for factors such as the complexity of the PDE to be solved, which surely influence the generalization capability of a neural network. We leave those two components out of the scope of this paper mainly because the activation function represents a hyperparameter with too many degrees of freedom and requires a per-se study, while the complexity of the target function is an external component that we are not supposed to know a priori when training a PINN.

3 Preliminary Numerical Analysis

This section aims to provide numerical results to showcase and clarify the relevant features of a PINN architecture. Namely, we define the equation considered as a baseline for the upcoming study. Thereupon, we employ PINNs to solve said equation and use the trained architecture to highlight the main difference between PINNs and classical PDE solvers. Then, we use the same test case to clarify the issues of the generalization potential of a PINN, which is the core focus of this research.

For our scope, and without loss of generality, we choose a one-dimensional Poisson equation with a source term in the domain $[-\pi, \pi]$, presented in Equation (4), as an academic example to showcase and analyze the output of a trained PINN. The presented equations are also solved through PINNs in [24]. Such a choice for the equation relies on the richness of frequencies included in its solution, to have a target function that carries enough complexity. Moreover,

training PINN architectures is also extremely efficient in one dimension, which facilitates the analysis provided in this paper.

$$\begin{cases} \frac{\partial^2 u}{\partial x^2} = f & x \in [-\pi, \pi] \\ u(-\pi) = u(\pi) = 0 \end{cases}. \quad (4)$$

With $f : \mathbb{R} \rightarrow \mathbb{R}$, the source term, being defined as:

$$f(x) = \sum_{k=1}^5 2k \sin(2kx) \quad (5)$$

The correct solution of this equation can be easily derived analytically by integrating twice the source term in $[-\pi, \pi]$ and setting the integration constants to zero, in order to match the desired values at the boundaries. The function resulting from this operation and solution to Equation (4) is then given by:

$$u(x) = \sum_{k=1}^5 \frac{1}{2k} \sin(2kx) \quad (6)$$

To train the PINN architectures, we sample 100 collocation points in the domain $[-\pi, \pi]$ with the Latin hypercube sampling strategy and use a two-layers neural network architecture with 50 neurons per layer and hyperbolic tangent as activation function. To train the model we restrict it to 10000 iterations of the Adam optimizer [25], followed by the L-BFGS optimizer [26] to fine-tune the results, limited to 10000 iterations and a tolerance of 10^{-8} . The training process takes a few minutes to converge to a solution and outputs predictions that are visually indistinguishable from the correct solution, which can be seen in Figure 1.

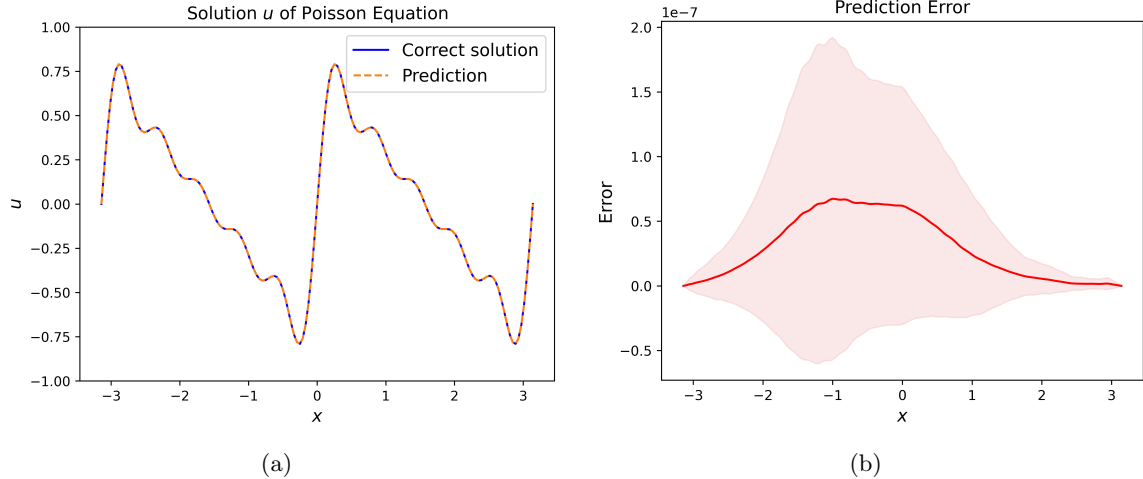


Fig.1: Correct versus predicted solutions (a) and relative L^2 error (b) for 100 randomly initialized and trained PINN architectures. Variance is also included in both figures but it is too small to be visible in (a).

In the same way, we used automatic differentiation to compute the equation residuals, we can also use it to access the derivatives of u_θ and compare them with the true ones. Due to the

PDE that we are solving, it is already known that the prediction of the second derivative of u will be accurate. Therefore, we compute and showcase the comparison of derivatives up to the fourth order along with the related relative L^2 error made in prediction. The choice of using the relative error rather than the classical squared error used in the previous section is due to the difference in magnitude of the values of u and its first four derivatives, which goes from unitary order to 10^3 . The results are shown in Figure 2. Again, it is barely possible to distinguish the correct values from the ones obtained through the PINN architectures.

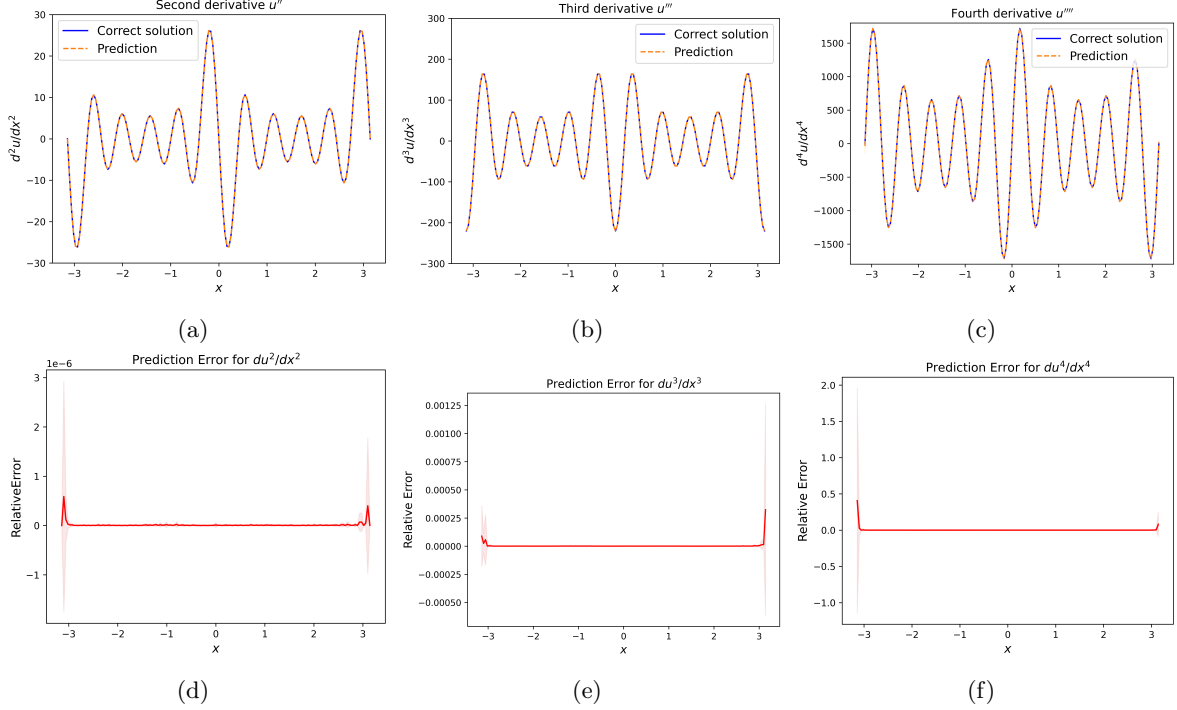


Fig. 2: True vs predicted values for the second, third and fourth derivative of the target solution for five randomly initialized and trained PINN architectures (respectively a,b, and c) along with their respective relative L^2 errors in prediction (d, e, and f). Variance of the prediction is also included but almost undistinguishable.

3.1 Generalization beyond the Training Domain

We now proceed to investigate the concept of generalization for a PINN architecture expressed in Section 2. Instead of solving Equation (4) in the whole domain, we now restrict the training to subsets, to evaluate the behavior of the predicted solution outside the training domain. We first split the training domain into three smaller domains, namely $\Omega_1 = [-\pi, -\frac{\pi}{3}]$, $\Omega_2 = [\frac{\pi}{3}, \frac{\pi}{3}]$, and $\Omega_3 = [\frac{\pi}{3}, \pi]$ and perform training of 100 randomly initialized PINN architectures with identical structures, in order to grasp the effect of stochasticity in the training procedure. From an analytical perspective, the exact solutions u^j solving Equation (4) in the respective subdomains Ω_j are all represented by the same function, due to the uniqueness of the solution. This would mean that each u_θ^j in each Ω_j should behave the same in the whole Ω , which is not the case in practice. Based on the continuity of u_θ and the target function, the only fair assumption is that the PINN prediction will shortly follow the analytic function. The results plotted in Figure 3 show the behavior described above, along with the degradation of prediction outside the training area.

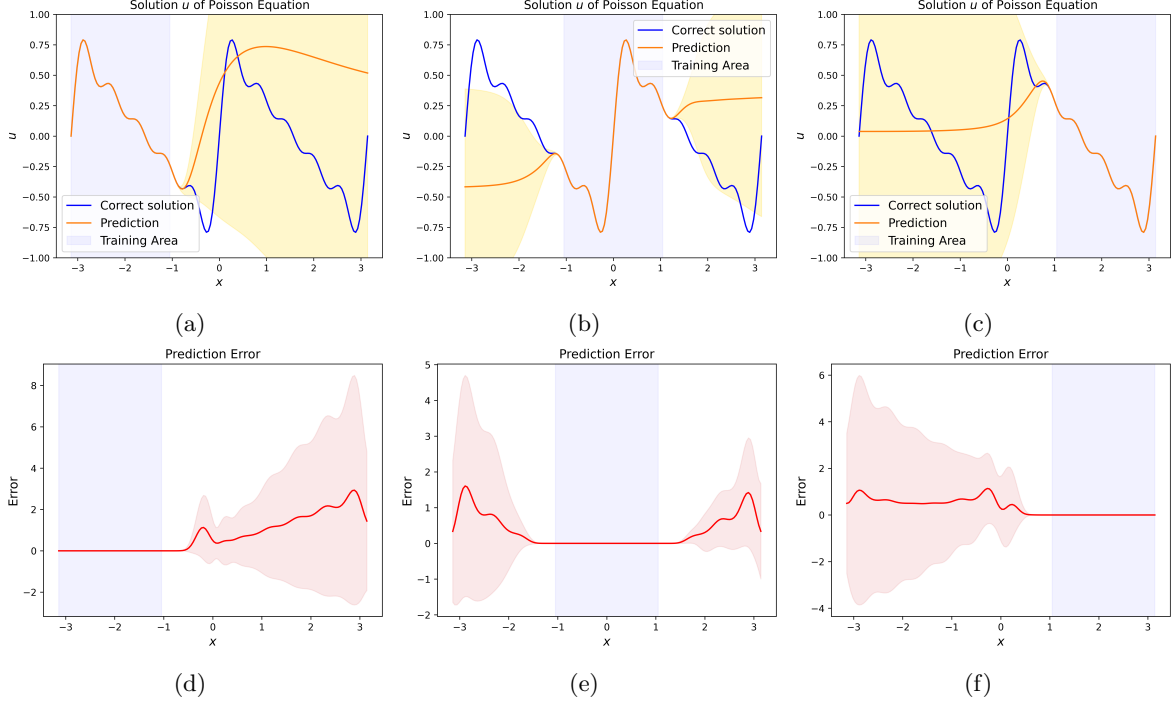


Fig. 3: Prediction and ground truth (a,b,c) and related error (d,e,f) for PINNs trained in the respectively light blue area. The shaded gold and red areas represents two times the standard deviation of the prediction and the error of PINNs respectively.

As expected, predictions are extremely accurate in the training area and maintain precision right outside of it. Indeed, since the network is able to properly approximate the derivatives of the target function at some point, then it can also approximate the target function properly in a ball around said point. However, the prediction quickly becomes unreliable and subject to stochasticity further away from the training domain. Indeed, the average PINN prediction suggests that no accurate function evaluation can be done with confidence outside the convex hull defined by the collocation points used in training. The same concept is expressed through rigorous analytical error bounds in [16, 27], where the tightest error estimates present an exponential increase in time when moving far away from the training area. However, the behavior of the PINN outside the training domain can be used as an insight into which algorithmic choices can make the network more suitable to learn the PDE.

4 Hyperparameter study through the Generalization Level

In this section, we provide numerical results on the power of generalization for various hyperparameters of the PINN algorithm. The results obtained for the G_l metric are presented alongside training time information, to provide a more complete understanding of the benefits of specific parametric settings. Moreover, for each hyperparameter, we also provide further visualizations of the behavior of the predictions when the related hyperparameter changes. For all hyperparameter analysis, we perform training of 100 randomly initialized PINN architectures restricted to 5000 Adam iterations with learning rate 10^{-3} and a subsequent L-BFGS optimizer limited to 5000 iterations and 10^{-8} tolerance. The results are then thoroughly discussed in Section 5.

4.1 Network Complexity

The first case taken into consideration is the complexity of the network adopted to define the PINN architecture. The analysis is divided into the number of neurons and the number of layers, to properly grasp the effect of each of the two components.

Number of Neurons We consider the number of neurons of single-layered neural network architectures. We test several PINN architectures characterized by the number of neurons of their single hidden layer and evaluate them based on the value of the GL metric. In order to fully grasp the effect of under and over-parametrized regimes, we test architectures with 10, 20, 50, 100, 200, 400, and 600 neurons. The results obtained for this analysis are shown in Figure 4, along with the average training time per architecture configuration and its variance.

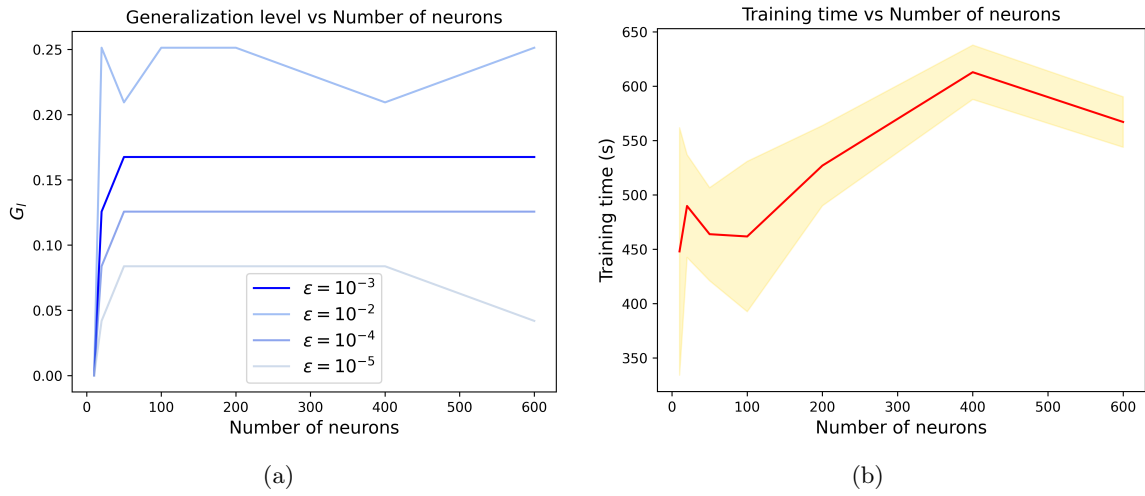


Fig. 4: G_l values for different values of ϵ when the number of neurons is increased (a) and training time (mean and variance) of each training configuration (b).

Regarding the value of the generalization metric, the value is always zero for the smallest architecture since, on average, 10 neurons are not enough to learn the target function. Increasing the number of neurons rapidly enhances the generalization power of the architecture, which seems to be generally saturated as soon as 50 neurons are used. When the number of neurons is further increased, no clear enhancement is obtained in terms of the generalization metric we have defined. The training time, on the other hand, presents a more peculiar behavior. As expected, convergence is faster on average for smaller architectures, but the variability of the training time is instead much larger. The choice of a 50 neurons architecture seems to be the most appealing both in terms of average training time and variability.

In Figure 5, it is possible to also visualize the impact on prediction when the number of neurons in a single-layer architecture is increased. Increasing the width of the network seems to generally skew the outside prediction to an overestimation by the PINN, leading to a solution that rapidly departs from the correct one. This effect is not clearly visible for a relatively small number of neurons – 10, 20, and 50 – and becomes quickly more remarkable when the over-parametrization regime is reached. It is also interesting to notice that the over-parametrization regime does not appear to be beneficial to predict the solution of a PDE, at least in terms of the width of the network.

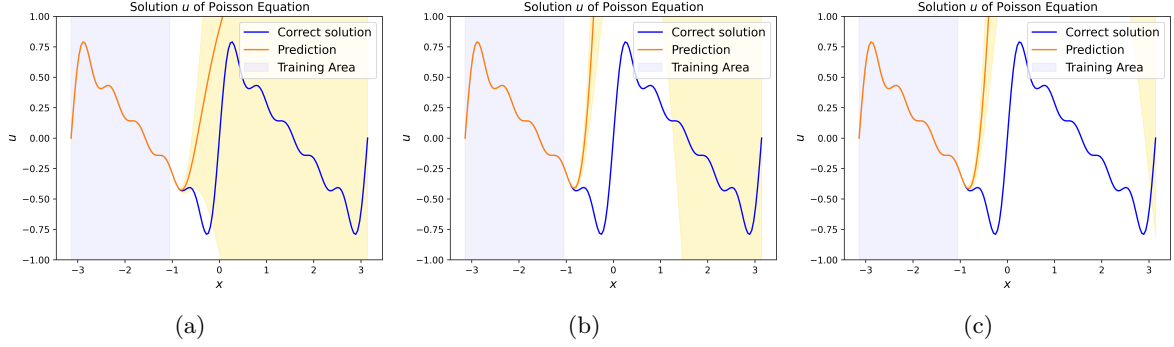


Fig. 5: PINN predictions (with variance) and ground truth for single layer architectures with 20(a), 400(b) and 600(c) neurons, trained in the light blue area.

Number of Layers An analogous analysis is conducted for neural architectures with a fixed number of neurons and a variable number of layers. We provide our analysis with as many as 50 neurons per layer and study architectures with 1, 4, 10, and 20 layers. Once more, the results are presented along with the statistics of the training time per network architecture and can be seen in Figure 6.

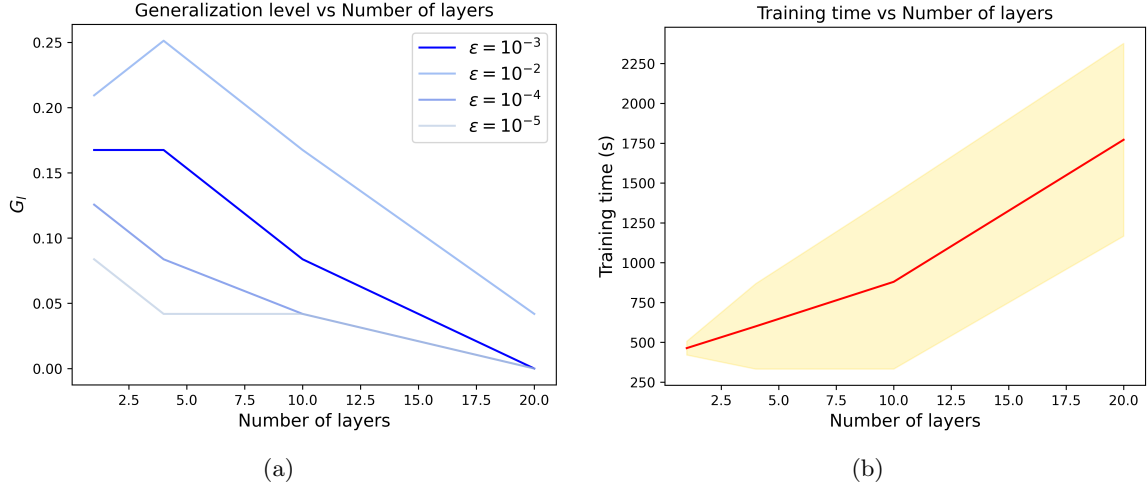


Fig. 6: G_l values for different values of ϵ when the number of hidden layers of the network is increased (a) and training time (mean and variance) of each training configuration (b).

The results obtained for the generalization level show on average a decay of the metric value when the number of layers is increased. The exception is the case of five layers or less, where it is possible to notice a slight improvement in the metric for some ϵ . It is also noticeable that the deepest architecture – 20 layers – gives almost always zero as generalization metric: this is due to the fact that the training process consists of a limited number of iterations and is stopped afterwards. The number of epochs is not enough to have such a big architecture converge properly. However, we noticed that even when trained for longer periods, such deep architectures struggle to achieve a suitable solution and do not achieve relevant results in terms of the generalization level. Moreover, the results obtained for the training time show an almost linear increase for the average training time, while its variability is significantly smaller when the number of layers is small.

In Figure 7, we also provide a visual representation of the effect on the predicted solution of an increasing number of layers. The depth of the PINN appears to smoothen out the

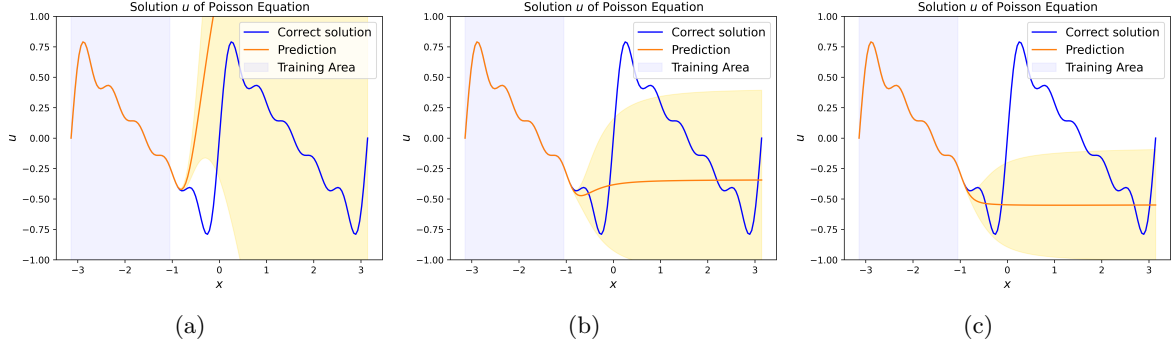


Fig. 7: PINN predictions (with variance) and ground truth for architectures with 1(a), 4(b) and 10(c) layers and 50 neurons per layer, trained in the light blue area.

prediction of the network to a constant value outside the boundary of the training domain. Moreover, this smoothened guess seems to have reduced variability when more layers are added. This impacts the GL metric negatively since its value is based on the outcome of the worst-performing architectures among all the trained ones.

4.2 Number of collocation points

We perform our routine analysis on single-layered neural network architectures with 20 neurons, which take as training input a variable number of collocation points. In our setting we test the case of 18, 25, 36, 50, 100 and 200 collocation points randomly sampled in each iteration with the Latin hypercube sampling strategy over the training domain $[-\pi, -\frac{1}{3}\pi]$. The results obtained for the generalization level and the training time are given in Figure 8.

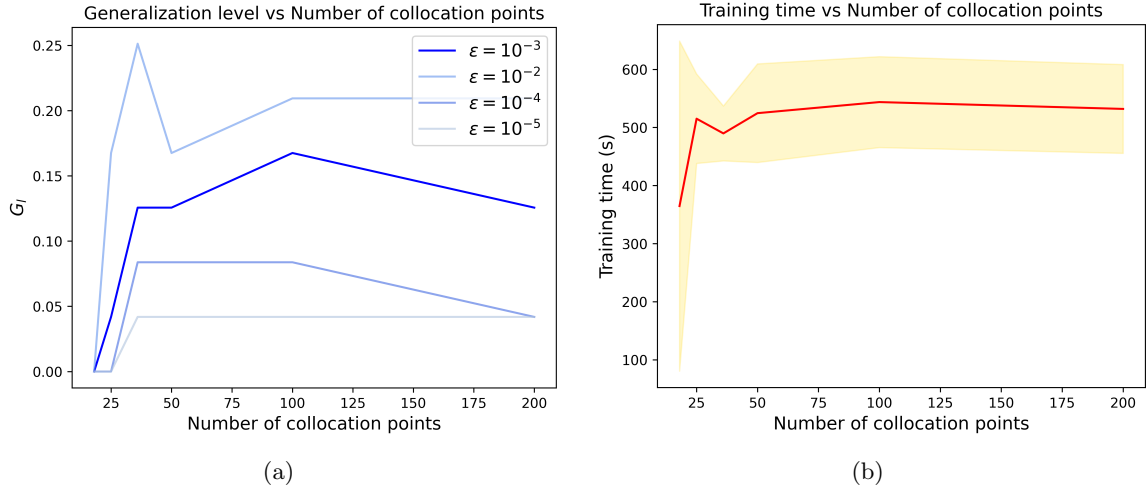


Fig. 8: G_l values for different values of ϵ when the number of collocation points is increased (a) and training time (mean and variance) of each training configuration (b).

The resulting values of our generalization metric show that 18 collocation points are not enough to learn the target function. Once the number of collocation points is increased, the value of the generalization metric also increases. Overall, the generalization level is not largely affected by the number of collocation points used, as long as enough points are provided. Moreover, for the case used in our analysis, 36 collocation points are sufficient to learn the target function and obtain a good value of generalization. The training time presents a similar steady behavior with respect to the number of collocation points used for training, except

for the case when few points are sampled and the training does not reliably converge to the correct solution.

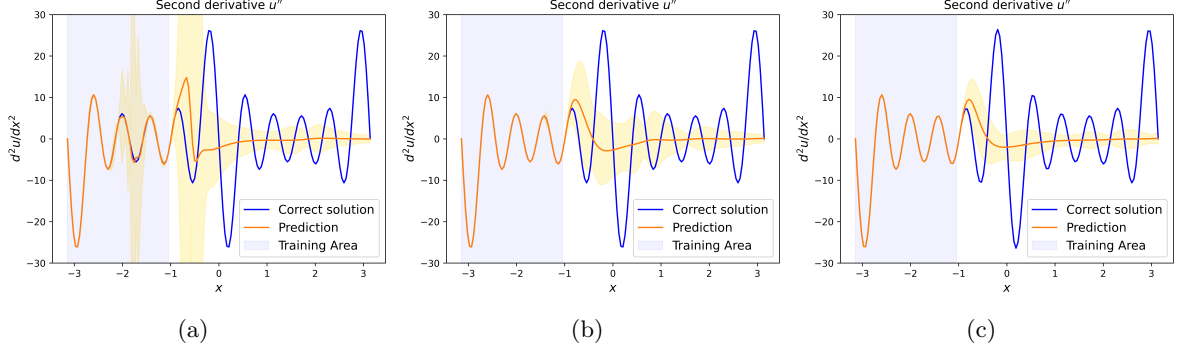


Fig. 9: PINN predictions (with variance) and ground truth of the second derivative of the PDE solution for architectures trained with 18(a), 25(b) and 36(c) collocation points distributed in the light blue area.

Furthermore, the number of collocation points does not present any major pattern in the prediction of the PDE solution. The only visible effect can be noticed in the prediction of the second derivative of the target function in the low numbers regime. The latter is provided in Figure 9, which includes the prediction results of the second derivative for PINNs trained with 18, 25, and 36 collocation points sampled in the training domain. In this visualization, it is possible to see that an increased number of collocation points reduces the variability of the predictions outside the training area. Among those architectures, the latter configuration is the only one that completely reached convergence, as it is possible to identify a non-zero variance in the predictions obtained via training with both 18 and 25 collocation points.

4.3 Domain Size

With domain size, we refer to the length – or area – of the region where the collocation points are sampled and where the underlying PDE is defined. For the analysis of this Section, we consider decreasingly smaller domains that are defined as $\Omega_i = [-\frac{1}{3}\pi - \frac{2}{3 \cdot 2^i}\pi, -\frac{1}{3}\pi]$ for $i = 0, 1, 2, 3, 4$. Since we have already studied the effect on the generalization of the density of CP in the training domain, we reduce the number of collocation points picked for training the network coherently with the decrease in the size of the domain. The network architecture, instead, is kept fixed to a single-layered neural network with 20 neurons, to properly grasp the effect in generalization of the domain size. For the sake of comparability, the value of the GL metric is computed for the right side of the outer domain, which means that is computed for all training setups in the area where $x \geq -\frac{1}{3}\pi$. The results for the generalization metric and training time are shown in Figure 10.

Regarding the generalization level, we can see that the architectures trained on the smallest domain generalize poorly to points outside Ω_T . This is mainly due to the fact that the network is not able to properly grasp the complexity of the whole target function in such a small area. Indeed, the GL values obtained in our analysis show an initial increase with the domain size and thereafter a clear decay with respect to the size of the domain. On the other hand, the training time presents an interesting behavior as well: an increased time demand for larger domains on average, but a much larger variability in training time for the intermediate values tested. This is most likely due to the richer variety of functions which presents the behavior

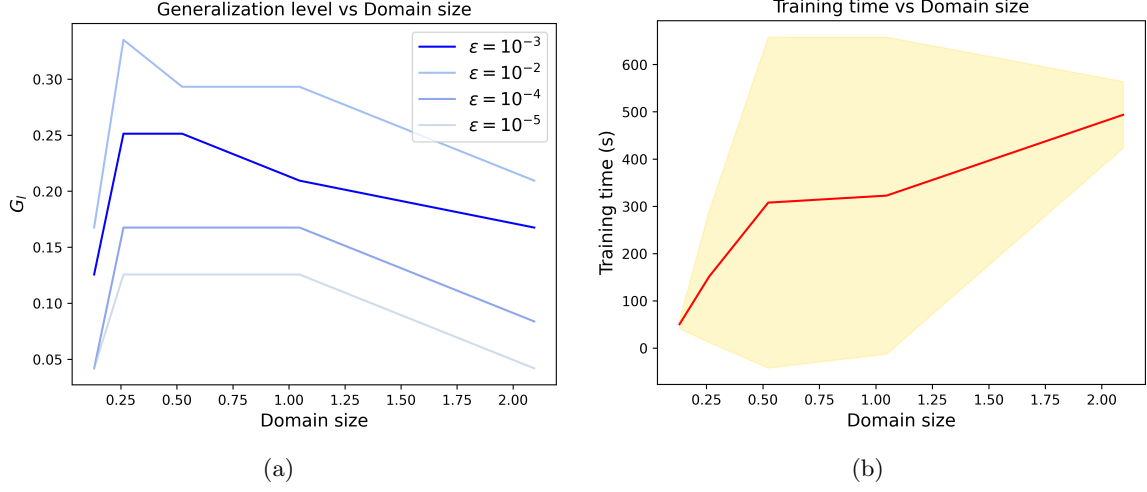


Fig. 10: G_l values for different values of ϵ when the size of the training domain is increased (a) and training time (mean and variance) of each training configuration (b).

described by the PDE residuals in the training domain. The case of the smallest domain represents once more an exceptional case, for which the training time presents a substantially small variance.

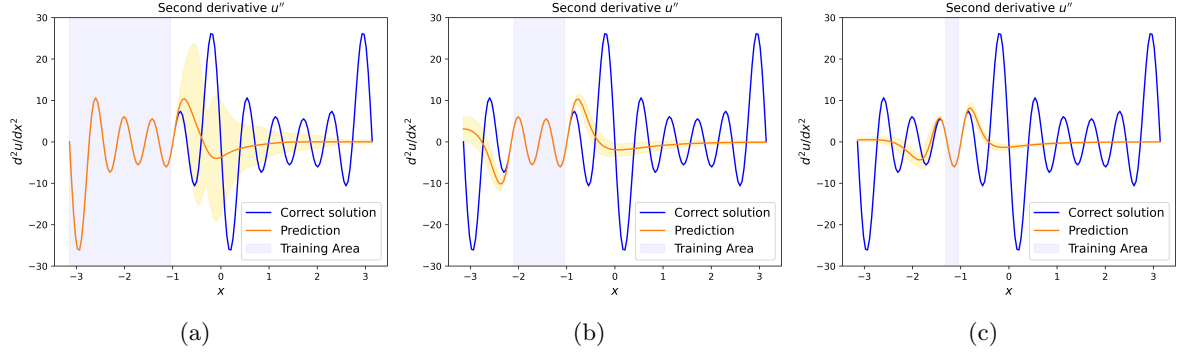


Fig. 11: PINN predictions (with variance) and ground truth of the second derivative of the PDE solution for architectures trained on the domain highlighted by the light blue area.

The case of the domain size also represents one of the most interesting impacts on the outcome of the prediction. For visual purposes, we present the effect of the domain size in terms of the prediction of the second derivative of the PDE solution. The results can be seen in Figure 11 for decreasing domain sizes. It is possible to notice that the main impact on predicting in small domains is given by a reduced variability of the prediction outside of the training area. Since the metric we defined evaluates the best-worst result, the variability of the prediction is a very impactful factor in its value.

4.4 Statistical Analysis of the results

In this section, we provide an additional analysis of the results obtained so far through statistical tests. In particular, we want to identify whether the differences in generalization levels for different architectural settings are statistically significant. To do so, we perform the Kruskal-Wallis H test for independent samples [21]. The latter sets as the null hypothesis the equality in the median of samples coming from multiple independent probability distributions. The

Kruskal-Wallis H test is based on the rank of the data samples and rejects the null hypothesis when one of the samples appears to have greater values than the other.

Moreover, the tests are not performed on the generalization level we defined, but rather on the value obtained before the minimization over u_θ of its definition in Definition 3. Therefore, for every neural network and every architectural and algorithmic setup, we consider the variable g_l , in Definition 7, as the subject of our statistical analysis.

$$g_l(u_\theta) = \max_{\Omega_G \subseteq \Omega \setminus \Omega_T} \{l(\Omega_G) \quad \text{s.t.}:: \|u(x) - u_\theta(x)\| \leq \epsilon \quad \forall x \in \Omega_G\} \quad (7)$$

Thus, for all the hyperparameters considered in our study, we perform the Kruskal-Wallis H tests in order to assess whether any of the evaluated hyperparameters produces a statistically significant effect on the generalization level of a machine learning model. The test results are presented in Table 1, where both the value of the H statistics is shown for each hyperparameter and each value of ϵ . In the aforementioned Table, we highlight the H values in bold when the p-value is above 0.01, which represent cases in which the H statistic can not validate any statistically significant difference.

Hyperparameter vs ϵ	$1e-3$	$1e-2$	$1e-4$	$1e-5$
N. of Neurons	183.46	238.15	206.35	235.19
N. of Layers	98.72	37.09	123.91	111.83
N. of CP	6.31	16.38	8.86	18.53
Domain Size	260.27	48.68	324.89	346.30

Table 1: Kruskal-Wallis’ H statistic value for all hyperparameters and all values of ϵ studied. Values in bold refer to cases where statistically significant differences can not be validated

Except for the number of collocation points used in training, all hyperparameters present a strong statistical significance, for any ϵ , to reject the null hypothesis of the Kruskal-Wallis test. This means that the values of g_l are directly influenced – with very high probability – by each of the hyperparameters considered in our study. To identify where the statistically significant differences appear within each group, we also perform pairwise Mann-Whitney U tests – the two-sample version of the Kruskal-Wallis test – for each of the hyperparameters that have shown statistically significant differences. The results obtained through these post-hoc tests can be summarized as follows:

- **Number of Neurons:** statistically significant differences seem to be present in blocks. Networks with 10 to 100 neurons appear to present similarities within each other, as do networks with 200 to 600 neurons. However, the null hypothesis is always rejected between the two groups, regardless of the values of ϵ .
- **Number of Layers:** similar to the case of the number of neurons, results obtained for architectures with 4 or more layers appear to be correlated, while the null hypothesis is always rejected between the one-layered architecture and the other networks.
- **Domain Size:** The null hypothesis is always rejected, except for the two configurations with larger domain size, which seem to be correlated when ϵ is very small.

Finally, we can conclude that varying the number of collocation points does not influence the generalization level of a PINN. On the other hand, the network complexity and the size of

the PDE domain have a statistically significant impact on the value of the generalization level.

5 Discussion on the effect of the algorithmic setup

In this section, we analyze the results obtained in this paper to provide further insights into the effect of the investigated hyperparameters on the generalization of a PINN. We first briefly comment on the results obtained in our preliminary analysis of Section 3 and then focus on the effect on the generalization level and training time of each of the hyperparameters individually. We present the aforementioned results along with additional highlights that were noticed during the training of all the PINN architectures used in this paper and in comparison with the research literature.

Our preliminary analysis highlights how a PINN solution represents an accurate approximation of the whole target PDE solution u , including its derivatives. This property of PINNs is particularly interesting because it represents the most consistent difference between a PDE solution obtained with a classical solver. Indeed, extrapolating the solution outside of a mesh is performed through interpolation of the values obtained on the mesh. The order of this interpolation can be arbitrary and is also strictly related to the numerical scheme used to solve the discretized PDE. Therefore, high-order derivatives might not be computable when we solve a PDE through classical methods, while a PINN architecture aims to fully mimic the solution u , even in its high-order derivatives. On the other hand, our analysis clearly shows that a PINN understandably fails to learn the analytical extension of the PDE solution in regions that do not contain any of the collocation points used during training. However, the architecture maintains the accuracy obtained inside the training domain when predictions are made in the proximity of its boundaries. This is due mainly to the smoothness of both u and u_θ and means that a PINN architecture has a – very limited – potential to approximate the target function even outside the training domain. Therefore, the outcome of our study is given by which settings should generally be considered good practice when utilizing a Physics-Informed Neural Network architecture.

Network Complexity We notice that increasing the width of the network skews the prediction to overestimated results. However, the value of the generalization metric is not largely affected by the width of the network. Generally, when training an arbitrary neural network, it is common practice to over-parametrize the latter to be sure that the network can capture the complexity of the target function. This is a recently noticed behavior of neural networks in the overparametrized regime which is regarded in the scientific community as the double descent phenomena [15]. Curiously, the latter is not clearly visible when considering the generalization level introduced in this project. Neural networks are also subject to implicit bias [31] which skews them towards learning simple solutions. However, the results obtained so far hint that a smaller architecture might be more suitable for training a PINN as computational time is larger for wider architecture while the generalization level does not largely improve. In particular, the only disadvantage of using a smaller architecture is given by the uncertainty of the capacity of the defined PINN to solve the PDE, whilst an over-parametrized architecture is generally more reliable in these terms.

Increasing the depth of the network skews the PINN to return a flat prediction outside the training domain, which suggests that no information is somehow gathered from the inner domain. Moreover, the generalization level is worsened by the depth, and training time is visibly increased without additional benefits. Therefore, the evaluation metrics considered in this paper suggest that a shallow and thin architecture is a more suitable choice for the architecture of a PINN. This concept holds specifically for the relatively simple PDE considered as a base case. Therefore, the results obtained do not imply that a smaller network is always a more suitable solution, but rather that it is possible and advantageous – in terms of generalization level and training time – to compute relatively simple PDE solutions via a PINN with few trainable parameters.

Number of collocation points The generalization level is not largely affected by the number of collocation points. This implies that if the collocation points sampled are enough to correctly predict the target function, there is no benefit in adding more, except for cases of adaptive sampling [22]. Moreover, it is also worth noting the unexpected increase in the variability of training time when few collocation points are given. This is most likely related to the fact that using few points generates several local minima in the loss landscapes which are seen as acceptable to the algorithm. However, the lack of impact in training time is most likely because the computational overhead created by just 200 collocation points is negligible for a use case like the one we consider, for which the computation of the residuals is extremely fast. Nevertheless, this is not always the case, especially for multidimensional and highly non-linear equations such as Navier-Stokes’.

Domain size In terms of generalization level, we notice that training on a small domain appears to be beneficial for the PINN architecture. Indeed, the generalization level decays when the size of the training area increases, except for the smallest domain considered. As previously mentioned, for such a case, the chosen area does not capture enough complexity of the underlying function and therefore does not let the algorithm learn a function that generalizes well in the proximity of the training frontier. The numerical value of the generalization level obtained for the best-performing domain sizes is also rather surprising. Indeed, the values obtained indicate that the longest segment in which all architectures generalize well is just as big as the domain used for training – on the right side –. This means that, by training in the selected domain, we get the correct solution in a domain twice the size – even larger if we consider the generalization level on the left side as well –.

In general, training a PINN architecture is slow and difficult. However, as for the case of a few parameters, we noticed that the PINN training is at times incredibly fast, comparable with the case of the smallest domain size considered in our analysis. The results obtained are coherent with the available literature: indeed, PINNs are known to struggle when learning functions defined in big domains [29,33] and their training can be eased by learning on collocation points which are given sequentially to the algorithm [28,30]. In fact, learning on smaller domains requires a surprisingly short training time which also presents an extremely low variability. Since the architecture used is unchanged and the generalization metric actually improves, this could be due to the fact that a smaller domain acts as a regularization term, which skews the learning toward a specific solution in the search space of the neural network. However, this is not always true because the loss minimization problem of the PINN becomes harder

to solve since the number of worthy local minima in the loss landscape is reduced [32]. This is important to note as prediction variability largely influences the value of the generalization level.

5.1 Extension to different cases and higher dimensions

The results obtained in this paper can be extended to any kind of partial differential equations. In particular, if the considered PDE is monodimensional, it is rather straightforward to repeat the tests performed in our analysis. On the other hand, extending our analysis to PDEs in higher dimensions can be non-trivial conceptually and, more specifically, computationally.

Conceptually speaking, the proposed generalization level G_l represents the value of some distance d of data points from the convex hull of the training samples. When new unseen samples are fed to the model, the predicted value is guaranteed to be precise – up to a suitable threshold ϵ –, provided that the new samples are at most G_l away from the training data. In machine learning applications, it is fundamentally hard to guarantee a certain precision, as the underlying problems are typically affected by stochasticity. Thus, any guarantees are typically possible only with high probability and are not necessarily true in general. However, stochasticity should not appear when the underlying problem is the solution of a PDE, which is why we adopted a definition for G_l that should minimize the stochasticity intrinsic in a neural network architecture.

Based on the considerations above, it is possible that for different settings it is better to consider an alternative formulation of the generalization level which does not focus on the maximal set where a suitable generalization is achieved, but rather on the distance from the training set within which every prediction remains accurate. From the perspective of Definition 3, instead of searching for the maximal set $\Omega_G \subseteq \Omega \subseteq \Omega_T$, the aforementioned alternative should focus on a maximal distance value d_M , computed through some point-to-set distance d such as the Wasserstein distance. Such a metric can be defined as in Definition 8.

$$G_{l,\text{alt}}^\epsilon(\Theta, H) = \min_{u_\theta} \left\{ \max_{d_M} \left\{ d_M \quad \text{s.t.: } \forall x \quad d(x, \Omega_T) \leq d_M \implies \|u(x) - u_\theta(x)\| \leq \epsilon \right\} \right\} \quad (8)$$

Using either formulation of G_l is equivalent when the underlying problem is monodimensional. However, for higher dimensions, the two metrics can return many different results as Definition 3 allows for arbitrary complex shapes of Ω_G , whose area represents the metric value, while Definition 8 substantially limits the shape of Ω_G to that of a ball around Ω_T . However, the latter formulation represents a computational advantage over the former since it does not require approximating the area of an arbitrarily complex shape.

6 Conclusion

The initial goal of this paper was to shed light on the concept of generalization for a PINN and evaluate the prediction of said algorithm outside of its training domain. However, the majority of the well-known metrics for evaluation focus on the accuracy of the prediction, which can be misleading due to problem-specific requirements. Via the experimental settings defined

in this paper, we created an alternative method for evaluating the performance of a neural network based on its generalization capability and applied it to the case of PINNs. Through an academic example, we showcased the limits of PINNs in global generalization and, afterward, we analyse whether some experimental settings naturally influence it. By considering the training time, the effect on the prediction, and our metric, we obtained insights into which is the most naturally favorable algorithmic setup for solving a specific PDE with PINNs.

The results obtained with our metric showed counterintuitive results that are aligned with the scarce theoretical background available for PINN architectures. The majority of the hyperparameters studied have shown to impact the parametrization learned by the PINN training, either in the generalization level or in training time. Despite their effects being sometimes relatively small, the changes in the neural network’s output are generally visible. For instance, based on the results shown in this paper, the recently worshipped concept of overparametrization of neural networks might not be the most efficient choice when applying PINNs. Indeed, our analysis highlighted the advantages of using shallow and thin architectures, especially to learn PDE solutions on small domains. The latter fact underlines the potential of combining domain decomposition techniques with PINNs when solving a PDE, which is an approach already studied in papers as [34], but did not gather the attention it deserves.

Regarding the usage of the generalization level, future work should provide further results in terms of the generalization level for additional one-dimensional cases, such as a transport and/or advection-diffusion equation. The goal of performing such analysis would be to further validate the results obtained in this paper and explore additional insight into the training of PINNs based on the kind of differential equation that should be solved. An additional interesting research direction is given by the extension of the generalization level G_l to higher dimensions, to enable the application of the metric to more general non-physics-informed architectures and possibly connecting it to existing metrics for the generalization error of arbitrary models.

Based on the results obtained in this paper, future research on the PINN architecture should be skewed in directions that recall divide-and-conquer approaches as the one described in [35]. Another valuable alternative is represented by methods that consider sequential training as intrinsic to the architecture, as in [33]. Such extensions of PINNs should be accompanied by additional research on optimal neural network design and training setup. Further studies on all the hyperparameters involved in the training of a PINN should also be conducted, in order to develop a better understanding of this promising architecture.

Acknowledgements

We acknowledge the financial support of BMW AG, Digital Campus Munich (DCM), through the ProMotion program. This project was also funded by the Basque Government: KK2020/00049 project through ELKARTEK program, and the BERC 2022-2025 program. The Spanish Ministry of Science, Innovation and Universities is also acknowledged for its support through project PID2019-104966GB-I00 and through BCAM Severo Ochoa excellence accreditation CEX2021-001142-S/MICIN/AEI/10.13039/501100011033.

References

1. M. W. M. G. Dissanayake, and N. Phan-Thien, “Neural network-based approximations for solving partial differential equations”, *Communications in Numerical Methods in Engineering* 10(3), 195–201, 1994
2. I.E. Lagaris, A. Likas, and D.I. Fotiadis, “Artificial neural networks for solving ordinary and partial differential equations”, *IEEE Transactions on Neural Networks* 9(5), 987–1000, 1998
3. M. Raissi, P. Perdikaris, and G.E. Karniadakis, “Physics informed deep learning (part I): Data-driven solutions of nonlinear partial differential equations”, *arXiv preprint arXiv:1711.10561*, 2017
4. M. Raissi, P. Perdikaris, and G.E. Karniadakis, “Physics informed deep learning (part II): Data-driven discovery of nonlinear partial differential equations”, *arXiv preprint arXiv:1711.10566*, 2017
5. L. Yang, X. Meng, and G.E. Karniadakis, “B-PINNs: Bayesian Physics-informed neural networks for forward and inverse PDE problems with noisy data”, *Journal of Computational Physics* 425, 2021
6. P. Chuang, and L. A. Barba, “Experience report of Physics-informed neural networks in fluid simulations: pitfalls and frustration”, *arXiv preprint arXiv:2205.14249*, 2022
7. M. Raissi, A. Yazdani, and G. E. Karniadakis, “Hidden Fluid Mechanics: A Navier-Stokes informed deep learning framework for assimilating flow visualization data”, *Science* 367.6481 (2020): 1026-1030
8. G. Kissas, Y. Yang, E. Hwuang, W. R. Witschey, J. A. Detre, and P. Perdikaris, “Machine learning in cardiovascular flows modeling: Predicting arterial blood pressure from non-invasive 4D flow MRI data using Physics-informed neural networks”, *Computer Methods in Applied Mechanics and Engineering*, 358, 2020
9. B. Zapf, J. Haubner, M. Kuchta, G. Ringstad, P. K. Eide, and K. Mardal, “Investigating molecular transport in the human brain from MRI with Physics-informed neural networks”, *arXiv preprint arXiv:2205.02592*, 2022
10. K. Kashinath, et al., “Physics-informed machine learning: case studies for weather and climate modelling”, *Philosophical Transactions of the Royal Society*, 2021
11. Y. Xu, S. Kohtz, J. Boakye, P. Gardoni, and P. Wang, “Physics-informed machine learning for reliability and systems safety applications: State of the art and challenges”. *Reliability Engineering and System Safety*, 2022
12. G. E. Karniadakis, I. G. Kevrekidis, L. Lu, P. Perdikaris, S. Wang, and L. Yang, “Physics-informed machine learning” *Nature Reviews Physics*, 3(6), 422-440, 2021
13. M. Olson, A. Wyner, and R. Berk, “Modern neural networks generalize on small data sets”, *Advances in Neural Information Processing Systems* 31, 2018
14. M. S. Advani, A. M. Saxe, and H. Sompolinsky, “High-dimensional dynamics of generalization error in neural networks”, *Neural Networks Elsevier* 132, 428-446, 2020
15. S. Mei, and A. Montanari, “The generalization error of random features regression: Precise asymptotics and the double descent curve”, *Communications on Pure and Applied Mathematics* 75 (4), 667-766, 2022
16. S. Mishra, and R. Molinaro, “Estimates on the generalization error of Physics-informed neural networks for approximating a class of inverse problems for PDEs”, *IMA Journal of Numerical Analysis* 42 (2), 981-1022, 2022
17. E. Kharazmi, Z. Zhang, and G. E. Karniadakis, “hp-VPINNs: Variational Physics-informed neural networks with domain decomposition”, *Computer Methods in Applied Mechanics and Engineering* 347, 2021
18. B. Moseley, A. Markham, and T. Nissen-Meyer, “Finite Basis Physics-Informed Neural Networks (FBPINNs): a scalable domain decomposition approach for solving differential equations”, *arXiv preprint arXiv:2107.07871*, 2021
19. Y. Wang, X. Han, C. Chang, and D. Zha, U. Braga-Neto, and X. Hu, “Auto-PINN: understanding and optimizing Physics-informed neural architecture”, *arXiv preprint 10.48550/ARXIV.2205.13748*, 2022
20. M. Chaudhari, I. Kulkarni, and M. Damodaran, “Exploring Physics-Informed Neural Networks for Compressible Flow Prediction”, *Proceedings of 16th Asian Congress of Fluid Mechanics*, 2021
21. P. E. McKight, and J. Najab, “Kruskal-Wallis test”, *The corsini encyclopedia of psychology*, 2010
22. C. Wu, M. Zhu, Q. Tan, Y. Kartha, and L. Lu, “A comprehensive study of non-adaptive and residual-based adaptive sampling for Physics-informed neural networks”, *arXiv preprint arXiv:2207.10289*, 2022
23. R. Shama, and V. Shankar, “Accelerated Training of Physics-informed neural networks (PINNs) using Meshless Discretizations”, *arXiv preprint arXiv:2205.09332*, 2022
24. L. Lu, X. Meng, Z. Mao, and G. E. Karniadakis, “DeepXDE: A deep learning library for solving differential equations”, *SIAM Review* 63 (1), 2021
25. D. P. Kingma, and J. Ba, “Adam: A Method for Stochastic Optimization”, <https://arxiv.org/abs/1412.6980>, 2014
26. D. C. Liu, and J. Nocedal, “On the limited memory BFGS method for large scale optimization”, *Mathematical Programming* 45 (1), 503-528, 1989

27. T. De Ryck, A. D. Jagtap, and S. Mishra, "Error estimates for Physics-informed neural networks approximating the Navier-Stokes equations ", *arXiv preprint arXiv:2203.09346*, 2022
28. S. Mishra, and T. K. Rusch, " Enhancing accuracy of deep learning algorithms by training with low-discrepancy sequences ", *SIAM Journal on Numerical Analysis* 59 (3), 1811-1834, 2021
29. S. Wang, X. Yu, P. Perdikaris, "When and why PINNs fail to train: A neural tangent kernel perspective ", *Journal of Computational Physics* 449, 2020
30. A. S. Krishnapriyan, A. Gholami, S. Zhe, R. M. Kirby, and M. W. Mahoney, "Characterizing possible failure modes in Physics-informed neural networks ", *Advances in Neural Information Processing Systems* 34 (2021): 26548-26560
31. G. Valle-Perez, C. Q. Camargo, and A. A. Louis, " Deep learning generalizes because the parameter-function map is biased towards simple functions", *arXiv preprint arXiv:1805.08522*, 2018
32. F. M. Rohrhofer, S. Posch, C. Gößnitzer, and B. C. Geiger, " Understanding the difficulty of training Physics-informed neural networks on dynamical systems ", *arXiv preprint arXiv:2203.13648*, 2022
33. S. Wang, S. Sankaran, and P. Perdikaris, " Respecting causality is all you need for training Physics-informed neural networks ", *arXiv https://arxiv.org/abs/2203.07404*, 2022
34. A. Jagtap, and G. E. Karniadakis, " Extended Physics-Informed Neural Networks (XPINNs): A Generalized Space-Time Domain Decomposition Based Deep Learning Framework for Nonlinear Partial Differential Equations ", *AAAI Spring Symposium: MLPS*, 2021
35. H. Wang, R. Planas, A. Chandramowlishwaran, and R. Bostanabad, " Mosaic flows: A transferable deep learning framework for solving PDEs on unseen domains ", *Computer Methods in Applied Mechanics and Engineering* 389, 2022